University of Zurich[UZH]

Zurich Open Repository and Archive
University of Zurich
Main Library
Strickhofstrasse 39
CH-8057 Zurich
www.zora.uzh.ch

Year: 2017

Germline loss-of-function mutations in EPHB4 cause a second form of capillary malformation-arteriovenous malformation (CM-AVM2) deregulating RAS-MAPK signaling

Amyere, Mustapha ; Revencu, Nicole ; Helaers, Raphaël ; Pairet, Eleonore ; Baselga, Eulalia ; Cordisco, Maria ; Chung, Wendy ; Dubois, Josée ; Lacour, Jean-Philippe ; Martorell, Loreto ; Mazereeuw-Hautier, Juliette ; Pyeritz, Reed E ; Amor, David J ; Bisdorff, Annouk ; Blei, Francine ; Bombei, Hannah ; Dompmartin, Anne ; Brooks, David ; Dupont, Juliette ; González-Enseñat, Maria Antonia ; Frieden, Ilona ; Gérard, Marion ; Kvarnung, Malin ; Hanson-Kahn, Andrea Kwan ; Hudgins, Louanne ; Léauté-Labrèze, Christine ; McCuaig, Catherine ; Metry, Denise ; Parent, Philippe ; Paul, Carle ; Weibel, Lisa ; et al ; Vikkula, Miikka

Abstract: BACKGROUND: Most arteriovenous malformations (AVMs) are localized and occur sporadically. However, they also can be multifocal in autosomal-dominant disorders, such as hereditary hemorrhagic telangiectasia and capillary malformation (CM)-AVM. Previously, we identified RASA1 mutations in 50% of patients with CM-AVM. Herein we studied non-RASA1 patients to further elucidate the pathogenicity of CMs and AVMs. METHODS: We conducted a genome-wide linkage study on a CM-AVM family. Whole-exome sequencing was also performed on 9 unrelated CM-AVM families. We identified a candidate gene and screened it in a large series of patients. The influence of several missense variants on protein function was also studied in vitro. RESULTS: We found evidence for linkage in 2 loci. Whole-exome sequencing data unraveled 4 distinct damaging variants in EPHB4 in 5 families that cosegregated with CM-AVM. Overall, screening of EPHB4 detected 47 distinct mutations in 54 index patients: 27 led to a premature stop codon or splice-site alteration, suggesting loss of function. The other 20 are nonsynonymous variants that result in amino acid substitutions. In vitro expression of several mutations confirmed loss of function of EPHB4. The clinical features included multifocal CMs, telangiectasias, and AVMs. CONCLUSIONS: We found EPHB4 mutations in patients with multifocal CMs associated with AVMs. The phenotype, CM-AVM2, mimics RASA1-related CM-AVM1 and also hereditary hemorrhagic telangiectasia. RASA1-encoded p120RASGAP is a direct effector of EPHB4. Our data highlight the pathogenetic importance of this interaction and indicts EPHB4-RAS-ERK signaling pathway as a major cause for AVMs.

DOI: https://doi.org/10.1161/CIRCULATIONAHA.116.026886

Posted at the Zurich Open Repository and Archive, University of Zurich
ZORA URL: https://doi.org/10.5167/uzh-144457
Journal Article
Accepted Version

Originally published at:
Amyere, Mustapha; Revencu, Nicole; Helaers, Raphaël; Pairet, Eleonore; Baselga, Eulalia; Cordisco, Maria; Chung, Wendy; Dubois, Josée; Lacour, Jean-Philippe; Martorell, Loreto; Mazereeuw-Hautier,

Juliette; Pyeritz, Reed E; Amor, David J; Bisdorff, Annouk; Blei, Francine; Bombei, Hannah; Dompmartin, Anne; Brooks, David; Dupont, Juliette; González-Enseñat, Maria Antonia; Frieden, Ilona; Gérard, Marion; Kvarnung, Malin; Hanson-Kahn, Andrea Kwan; Hudgins, Louanne; Léauté-Labrèze, Christine; McCuaig, Catherine; Metry, Denise; Parent, Philippe; Paul, Carle; Weibel, Lisa; et al; Vikkula, Miikka (2017). Germline loss-of-function mutations in EPHB4 cause a second form of capillary malformation-arteriovenous malformation (CM-AVM2) deregulating RAS-MAPK signaling. Circulation, 136(11):1037-1048.
DOI: https://doi.org/10.1161/CIRCULATIONAHA.116.026886

10.1161/CIRCULATIONAHA.116.026886

Germline Loss-of-Function Mutations in EPHB4 Cause a Second Form of Capillary Malformation–Arteriovenous Malformation (CM-AVM2) Deregulating RAS-MAPK Signaling

Running Title: *Amyere et al.; Loss-of-Function Mutations in EPHB4 Causes CM-AVM2*

Mustapha Amyere, PhD & Nicole Revencu, MD, PhD, et al.

The full author list is available on page 14

American Heart Association.

Address for Correspondence:
Miikka Vikkula, MD, PhD
de Duve Institute
Université Catholique de Louvain
Human Molecular Genetics
Avenue Hippocrate 74
B-1200 Brussels Belgium
Tel: + 32-2-764 7490
Fax: + 32-2-764 7460
Email: Miikka.vikkula@uclouvain.be

Circulation

Downloaded from http://circ.ahajournals.org/ by guest on July 8, 2017

Abstract

Background—Most AVMs are localized and occur sporadically; however they also can be multifocal in autosomal dominant disorders, such as Hereditary Hemorrhagic Telangiectasia (HHT) and Capillary Malformation–Arteriovenous Malformation (CM-AVM). Previously, we identified *RASA1* mutations in 50% of patients with CM-AVM. Herein we studied non-RASA1 patients to further elucidate the pathogenicity of CMs and AVMs.

Methods—We conducted a genome-wide linkage study on a CM-AVM family. Whole exome sequencing was also performed on 9 unrelated CM-AVM families. We identified a candidate-gene and screened it in a large series of patients. The influence of several missense variants on protein function was also studied *in vitro*.

Results—We found evidence for linkage in two loci. Whole-exome sequencing data unraveled four distinct damaging variants in *EPHB4* in five families that co-segregated with CM-AVM. Overall, screening of *EPHB4* detected 47 distinct mutations in 54 index patients: 27 lead to a premature stop codon or splice-site alteration, suggesting loss of function. The other 20 are non-synonymous variants that result in amino-acid substitutions. *In vitro* expression of several mutations confirmed loss of function of EPHB4. The clinical features included multifocal CMs, telangiectasias, and AVMs.

Conclusions—We found *EPHB4* mutations in patients with multifocal CMs associated with AVMs. The phenotype, CM-AVM2, mimics *RASA1*-related CM-AVM1 and also HHT. *RASA1* encoded p120RASGAP is a direct effector of EPHB4. Our data highlights the pathogenetic importance of this interaction and indicts EPHB4-RAS-ERK signaling pathway as a major cause for arterio-venous malformations.

Key Words: arteriovenous malformation; arteriovenous fistula; capillaries; cardiovascular disease; vascular disease;

Downloaded from http://circ.ahajournals.org/ by guest on July 8, 2017

Clinical Perspective

What is new?

- Identification of a second type of capillary malformation-arteriovenous malformation (CM-AVM), named CM-AVM2.
- CM-AVM2 is characterized by intra/extra-cranial AVMs, multifocal CMs and telangiectasias.
- CM-AVM2 mimics RASA1-mutated CM-AVM1, but also hereditary hemorrhagic telangiectasia (HHT).
- Prevalence of CM-AVM1/2 is similar to that of HHT.
- CM-AVM2 is inherited as an autosomal dominant disorder.
- CM-AVM2 is caused by loss-of-function mutations in EPHB4.
- AVMs are caused by dysregulation of EPHB4-p120RASGAP (*RASA1*) interaction and downstream RAS-MAPK signaling.

What are the clinical implications?

- Patients with multifocal CMs need to be screened not only for an inherited RASA1 mutation, but also for EPHB4.
- Presence of telangiectasias may cause confusion with HHT.
- Screening of EPHB4 in HHT patients without a mutation in one of the 4 HHT genes and in patients with hereditary benign telangiectasia is to be considered to improve diagnostic.
- Risk for an intra-central system fast-flow lesion is lower than in CM-AVM1, but follow-up is needed.
- Inhibitors of EPHB4-p120RASGAP downstream signaling effectors, such as RAS and ERK, should be evaluated as possible molecular therapies for the management of AVM and CM.

Downloaded from http://circ.ahajournals.org/ by guest on July 8, 2017

Fast-flow lesions are characterized by direct communications between arteries and veins without an intervening normal capillary bed. In arteriovenous malformations (AVM), the arterial blood is shunted from the feeding arteries into the draining veins via a bundle of abnormal vessels, called the nidus. These lesions are usually congenital. Arteriovenous fistula (AVF) is another variant, in which communication between an artery and vein is direct, often caused by trauma. Multiple micro-AVFs are seen in Parkes Weber syndrome, in association with soft tissue and skeletal hypertrophy of the affected limb (OMIM 608355)[1].

AVMs can occur anywhere in the body; the central nervous system is the most common location. Symptoms depend on the site and age of the patient; e.g., fetal hydrops, cardiac failure, epilepsy and focal neurological deficit.[2] Progressive vascular dilation, potentially leads to rupture and hemorrhage.[3] AVMs are one of the most difficult to treat vascular anomalies and are associated with high morbidity and mortality.[2, 4, 5] They are highly dynamic with features of invasive growth, aggravation after incomplete resection, and regrowth even after clinically complete surgical removal.[6]

AVM can occur as an isolated feature or as part of a syndrome; the most common are hereditary hemorrhagic telangiectasia (HHT) and capillary malformation - arteriovenous malformation (CM-AVM). [7-10] HHT or Osler-Weber-Rendu syndrome (MIM187300) is a well-known autosomal dominant, genetically heterogeneous disorder, characterized by AVMs, typically in liver and lung, in association with cutaneous and mucosal telangiectasias. CM-AVM (MIM608354) is an autosomal dominant disorder with high penetrance and variable expressivity.[8] These patients have small multifocal cutaneous capillary malformations (CMs).[9-11] AVMs are seen in about 30% of the patients and are typically located in brain, spinal cord, face,

Downloaded from http://circ.ahajournals.org/ by guest on July 8, 2017

neck or extremities.[9, 10, 12] Parkes Weber syndrome is included in this disorder.[10] CM-AVM patients do not have frequent epistaxis, the hallmark of HHT.[3, 7, 12]

About one-half of the patients with CM-AVM have heterozygous loss-of-function mutations in *RASA1*.[9, 10] This gene encodes the cytoplasmic P120RASGAP protein, a negative regulator of the RAS signal transduction pathway that enhances the weak intrinsic GTPase activity of normal RAS p21.[13] P120RASGAP plays an important role in vascular development during murine embryogenesis[13, 14]. We studied several families that have phenotypical CM-AVM but without a *RASA1* mutation. Our hypothesis was that additional genes might be involved; we used linkage and whole exome sequencing to further unravel the pathogenetic cause of this disorder.

Downloaded from http://circ.ahajournals.org/ by guest on July 8, 2017

Methods

Recruitment of Patients

From our database of patients with vascular malformations, collected in our long-active research project, we culled 365 index individuals. Inclusion criteria were sporadic or familial CMs associated or not with fast-flow vascular malformations. All the participants or their legal guardians gave informed consent for the participation in the study. The ethnicity of the patients with an identified mutation (n=54) varied: Caucasian: 42, Hispanic: 7, North African: 3, Japanese: 1 and Chinese: 1. The research protocol was approved by the ethical committee of the medical faculty at Université catholique de Louvain, Brussels, Belgium.

Linkage Analysis

Molecular karyotyping was performed in all samples with Affymetrix Human Mapping 250K NspI according to the manufacturer's (Affymetrix) instructions

(Supplementary Methods). Genome-wide parametric multipoint linkage was performed using Merlin program12 in a large family with CM-AVM that did not have a *RASA1* point mutation or genomic rearrangement (CM-13-HO; **Supplementary Figure 1**). The parametric analyses were run under an autosomal dominant model, assuming a penetrance of 90% and 1% phenocopy rate. Haplotype reconstruction was used to exclude *RASA1* and to confirm segregation of the chromosome 7 locus with the CM-AVM phenotype in this family.

High Throughput Sequencing

Genomic DNA for one affected CM-13-HO family member and 10 patients from 8 additional families were used for whole exome sequencing. Exons were captured with Agilent SureSelectXT Human All Exon kit and sequenced with an Illumina HiSeq2000. We designed a custom AmpliSeq panel to sequence all exons and exon-intron boundaries of *RASA1* and *EPHB4* using the Ion PGM™ Sequencer. Called variants were annotated, filtered and visualized using Highlander, an in-house bioinformatics framework (Helaers and Vikkula, *submitted*; see URLs). Our sequencing methods, as well as variant filtering procedures, are described in the Supplementary Methods.

Effect of Non-Synonymous Variants on EPHB4 Function

Disease-causing variants were introduced in *EGFP-EPHB4* cDNA by site directed mutagenesis and transiently expressed in COS-7 cells. Stability of EPHB4 was accessed by Western blotting in cells treated or not with lysosome (Chloroquine) or proteasome inhibitors (MG132). Subcellular localization of EGFP-EPHB4 was evaluated by fluorescence imaging.

Statistical Analysis

To distinguish pathogenic mutations from background polymorphisms we evaluated the distribution of rare non-synonymous variants (NSVs) within the two genes, EPHB4 and RASA1.

Downloaded from http://circ.ahajournals.org/ by guest on July 8, 2017

Only NSVs with maximum allele frequency <0.003 in seven public databases (ExAC_af, 1000G_AF, ESP6500_AA_AF, ESP6500_EA_AF, gonl_af, ARIC5606_AA_AF and ARIC5606_EA_AF) were retained for analyses. NSVs were classified into tolerated or damaging on the basis of their aggregation score, as defined by Dong and coworkers.[15] These scores are based on nine prediction algorithms (SIFT, PolyPhen-2, GERP++, Mutation Taster, Mutation Assessor, FATHMM, LRT, SiPhy, PhyloP), the maximum frequency observed in the 1000 genomes database, and pre-computed with Logistic Regression (LR) for 87 347 044 possible variants in the entire human exome. Frequencies of tolerated (aggregation score: 0 - 0.49) and damaging (aggregation score: 0.5 - 1) NSVs in *RASA1* and *EPHB4* genes were compared between our patient cohort and control population on the basis of the largest public database ExAC[16] (60.706 unrelated whole exomes). As our study group consisted mainly of Caucasians (79,6%), we excluded individuals of other ethnicities from this analysis. Enrichment was estimated by Pearson's chi-square test: 2-sample test for equality of proportions with continuity correction (R-package v3.1.2).[17]

Downloaded from http://circ.ahajournals.org/ by guest on July 8, 2017

Results

Identification of *EPHB4* As the Mutated Gene

The genome-wide linkage analysis conducted with CM-13-HO family (**supplementary Fig.1A**) showed two noteworthy peaks with maximum LOD-scores of 2.5 and 2.8 on chromosomes 5 and 7, spanning 74.2 Mb and 59.1 Mb, respectively (**supplementary Fig.1B-C**). Whole exome sequencing revealed 4 damaging variants in 5 families in a single gene, *EPHB4* (**supplementary Table 1**). Subsequent targeted gene sequencing identified 47 distinct mutations in 54 index patients out of 365 sequenced: 9 were non-sense, 11 caused a frame-shift, and 7 altered a

consensus splice site. These 27 mutations suggested loss-of-function of EPHB4. Twenty variants lead to amino-acid substitutions predicted to alter protein function (**Fig. 1 and Table 1**). The mutations co-segregated with the phenotype in each family (**supplementary Fig.2**). A splicing defect was confirmed in mRNA for 2 variants in subjects for whom lymphoblasts were available. Moreover, the frequency of rare damaging non-synonymous variants (NSV) was significantly different between our study group and the large Exome Aggregation Consortium (ExAC) dataset; (*p-value* < 0.0001; **supplementary Fig.3**). This was not seen for *RASA1*, mutations in which are known to be STOP-gains, Indels or splice-site changes. The data fulfill all the criteria set up by MacArthur and colleagues on reporting on causality of sequence variants in newly identified genes.[18]

The identified mutations are scattered along EPHB4 (**Fig. 1**). As the most 5-prime premature STOP codon appears at amino acid position 12, there is a low likelihood for neomorphic or dominant-negative function. There was no genotype-phenotype correlation according to position or type of mutation. Thus, all mutations should lead to haploinsufficiency. In one family, the c.345_347delCTA mutation deleted a tyrosine-(115) in the EphrinB2 binding domain, suggesting that this interaction may be particularly important for EPHB4-EphrinB2 signaling (**Fig. 1**). Further evidence is a study of crystal structure of the ligand binding domain of EPHB4 in complex with the extracellular domain of ephrinB2[19]. Yet, several missense mutations (n=9/20) clustered within the catalytic domain of EPHB4, encoded by exons 14 and 15. We expressed four of them (p.E664K; p.C845R; p.R838W and p.R864W) and detected low level of mutant forms compared to the wild type (**Fig. 2A**). Inhibition of endosome-lysosome acidification stabilized EPHB4 expression, bringing it close to wild-type levels, whereas inhibition of proteasomal system had a very weak effect (**Fig. 2A**). The same effect was

Downloaded from http://circ.ahajournals.org/ by guest on July 8, 2017

observed when the two treatments were combined with protein synthesis inhibitors (data not shown). The typical membranous staining of EPHB4 (**Fig. 2A**) was not seen with mutant forms by immunofluorescence. Fluorescent vesicular inclusions without EPHB4 are detected only in mutant (**Fig. 2 C-F**). In summary, these findings underscore that the mutations induce loss of function of EPHB4.

Identification of Mutations in EPHB4 Allowed Clinical Characterization of a New Entity: CM-AVM2

We analyzed clinical data from the 110 individuals (54 index patients and 56 relatives) found to have an *EPHB4* mutation. Penetrance was high, 93% (n=102). Isolated multifocal CMs were identified in 34 families (63%). In the remaining 19 families (35%) at least one individual had an AVM in addition to CMs (**Table 1**). All affected subjects (n=102) had pink-to-red cutaneous CMs, usually multifocal; 10 patients had only one CM. About 25% of the CMs had a surrounding white halo believed to be caused by micro-AV-shunting as detected by to-fro murmur with a Hand-held Doppler instrument (**Fig. 3**). CMs were either present at birth or appeared later during childhood or adolescence, and were localized on the extremities, trunk or head and neck. Size varied from pinpoint to large lesions, up to 15 cm in diameter; the borders were usually geographic. The stains were homogenous or telangiectatic, sometime with a pale central zone. Bier spots were noted in 13 individuals (12%), and 16 (15%) had telangiectasias, especially on upper thorax and lips, or periorally. Only a few patients had recurrent epistaxis.

Fast-flow lesions were present in 20 individuals (18%): arteriovenous fistulae (AVF; n=1), AVM (n=12), and Parkes Weber syndrome (n=8) (**Fig. 3**). Three lesions were located in the central nervous system: vein of Galen aneurysmal malformations (n=2) and intraspinal arteriovenous fistula (n=1). One additional vein of Galen aneurysmal malformation was

Downloaded from http://circ.ahajournals.org/ by guest on July 8, 2017

identified in a fetus whose father carried an EPHB4 mutation, but fetal DNA was not available for analysis. The other AVMs were located in the face (n=8), and the extremities (n=1). One patient had 2 AVMs. The eight Parkes Weber lesions were located in the right arm (n=2), left arm (n=2), right leg (n=3) and left leg (n=1)(**Table 1**).

Discussion

In this study, we identified *EPHB4* as a second gene that is mutated in patients with capillary malformation-arteriovenous malformation. We propose to name this entity CM-AVM2 to differentiate it from CM-AVM1 caused by *RASA1* mutations. These vascular disorders have similar characteristics, but there are also differences, which are important for differential diagnosis. Both are characterized by multifocal CMs and increased risk for fast-flow vascular malformations. The CMs are usually small with a haphazard distribution. Bier spots are observed in both conditions, but are more frequent in CM-AVM2. Moreover, the large CMs in CM-AVM2 can have a pale central region. Telangiectasias, especially obvious on the lips, but also in the perioral region and on the upper thorax, are seen in CM-AVM2, but not in CM-AVM1.

Fast-flow vascular malformations occur in CM-AVM2 and in CM-AVM1; however, the overall risk is somewhat lower in CM-AVM2 (18% versus 31%). The frequency of Parkes Weber syndrome and cervico-facial AVM is the same between the two entities, 7%.[9, 10] In contrast, AVMs in the central nervous system were found in 3% of patients with CM-AVM2, compared to 10% of patients with CM-AVM1.[9, 10, 12] Of note, the 2 intracranial AVMs diagnosed in CM-AVM2 were vein of Galen aneurysmal malformations; another vein of Galen anomaly was diagnosed in utero. Thus, *EPHB4* is a supplementary gene to be considered in patients with this dangerous intracranial fast-flow lesion, often first detected prenatally.

Downloaded from http://circ.ahajournals.org/ by guest on July 8, 2017

Telangiectasias are a major feature of both HHT and Hereditary Benign Telangiectasia (HBT). They can cause confusion with CM-AVM2. HHT is a well-known autosomal dominant, genetically heterogeneous disorder with 4 causative genes identified and at least two other loci awaiting elucidation.[7, 20,21, 22] HBT is a rare autosomal dominant disorder of unknown etiology and characterized by widespread cutaneous telangiectasias. In contrast to HHT, these patients have neither epistaxis nor fast-flow vascular malformations.[20, 23-25] . The concurrence of CMs with telangiectasias in CM-AVM2 is a major clinical clue to differentiate it from HHT and HBT. In addition, the extra central nervous system fast-flow vascular malformations are different in CM-AVM2 from those in HHT. CM-AVM2 is associated with cutaneous, subcutaneous, muscular and bony AVMs in face and neck or extremities and Parkes Weber syndrome, whereas pulmonary and hepatic AVMs occur in HHT. Since not all HHT patients have pulmonary and/or hepatic AVMs, sequencing *EPHB4* in those without a mutation in one of the 4 HHT genes is indicated. It would also be interesting to test *EPHB4* in patients with HBT, as all the features in this disorder are observed in patients with CM-AVM2.

The prevalence of HHT is reported to be 1/5,000[26]. The Exome Aggregation Consortium (ExAC) dataset includes 10 loss-of-function mutations (premature STOP codons or strong splice site mutations) in 60,706 subjects, a prevalence of 1/6,000. Similar mutations are present 3 times in RASA1 and 5 times in EPHB4; thus prevalence estimates are 1/20,000 and 1/12,000, respectively. This calculation ignores all pathogenic amino acid substitutions. Overall, the prevalence of CM-AVM1/2 is similar to that of HHT1/2/3; and CM-AVM subtypes are strongly under-diagnosed.

Mutations in *EPHB4* were identified in 54 families. Most mutations were private to each affected family except for five mutations, which occurred in two families and one which

Downloaded from http://circ.ahajournals.org/ by guest on July 8, 2017

occurred in three families. The mutations are located throughout the gene; we found no genotype-phenotype correlations. The localized nature and multifocality of lesions in CM-AVM2 can be explained by the need for a somatic second hit for complete cellular abolishment of EPHB4 function. This two-hit phenomenon has been shown for other hereditary multifocal vascular malformations, such as CM-AVM1, glomuvenous malformations (GVM; OMIM 138000) and cutaneomucosal venous malformation (VMCM, OMIM 600195) [10, 27, 28,29]. The inherited mutation can be considered as a predisposing event, whereas additional genetic alterations disturb cellular function. No mutation was identified in 311 index patients. This negative finding was not unexpected taking into consideration the heterogeneity of our cohort, which includes patients with sporadic or familial CMs with/without a fast-flow vascular malformation. Moreover, regulatory regions were not analyzed.

The mechanism leading to CMs and AVMs in CM-AVM2 is likely a loss-of function of EPHB4. The majority of the mutations generate a premature stop codon, frame-shift or splice-site alteration (57%), leading to non-sense-mediated mRNA decay or an unstable and/or truncated protein. Moreover, our functional studies on several missense mutations, enriched in the catalytic domain of EPHB4, have shown reduced expression of mutant protein, caused by lysosomal degradation. As other inherited multifocal vascular anomalies have somatic second-hits, it is likely that the endothelial cells that drive formation of the lesions in CM-AVM2 are completely devoid of EPHB4 function. Unfortunately, we did not have tissue available to study this.

EPHB4 is a transmembrane receptor that is preferentially expressed in venous endothelial cells during vascular development.[30, 31] Its ligand, EphrinB2, is also a transmembrane protein, which is expressed in arterial endothelial cells.[32] This bidirectional signaling system, in concert

Downloaded from http://circ.ahajournals.org/ by guest on July 8, 2017

with Notch signaling, is a major controller of arterial-venous differentiation, especially via the forward signaling of EPHB4.[33,34] Coordinated activation of the two proteins is essential for establishment of venous and arterial endothelial identity and corresponding vessel formation (**Fig 4**).[33,34] EphB4-/- mice, as well as ephrin-B2-/- mice[30, 35], die at embryonic day E10.5, as a consequence of defects in peripheral angiogenesis, establishment of arteriovenous boundaries and vascular remodeling.[32]

EPHB4 signals via RAS/MAPK/ERK1/2 and PI3K/AKT/mTORC1 pathways.[36] In zebrafish, inhibition of EPHB4 or p120RasGap causes very similar vascular defects.[37] Moreover, EPHB4 with mutated conserved juxtamembrane tyrosine residues, abrogates the interaction with p120RASGAP, demonstrating that it is a pivotal effector of EPHB4 signaling.[38] The phenotypic similarity of CM-AVM1 and CM-AVM2 underscores this functional link, and incriminates dysregulation in EPHB4 signaling pathway as the cause of CM and AVM. Consequently, RAS and its downstream effectors, RAS/MAPK/ERK1/2 and PI3K/AKT/mTORC1, are constitutively activated (**Fig. 4**). ERK activation was observed in tissue samples from patients with RASA1 mutation.[37] Moreover, single somatic activating GNAQ/GNA11 mutations in sporadic CMs also activate these pathways.[39, 40] Thus, sporadic AVMs are likely caused by somatic activating mutations in (a) key molecule(s) of this signaling pathway as recently reported for 16 out of 25 patients with an extracranial sporadic AVM.[41]

The annual risk of hemorrhage associated with brain AVMs is about 2% per year.[42] The Randomised trial of Unruptured Brain Arteriovenous malformations (ARUBA) concluded that medical management is superior to endovascular interventional therapy alone for the prevention of death and stroke.[42] Extra-cranial AVMs present an equal therapeutic dilemma, with early complete surgical resection with/without embolization being the only hope for long-term

Downloaded from http://circ.ahajournals.org/ by guest on July 8, 2017

control.[43] Inhibitors of EPHB4-p120RASGAP downstream signaling effectors, such as RAS and ERK, should be evaluated as possible therapy for AVM, and CM.

In conclusion, we identified a hitherto unrecognized clinical entity, similar in clinical presentation to CM-AVM1 and, thus named CM-AVM2. Cutaneous CMs are highly penetrant and are associated with AVMs. Telangiectasias and epistaxis also occur, placing this novel disorder phenotypically between CM-AVM1 and HHT. The distribution of AVMs is more similar to CM-AVM1. CM-AVM2 is caused by loss-of-function mutations in EPHB4, whereas CM-AVM1 is due to loss-of-function of p120RASGAP. The latter has been demonstrated to be a direct effector of EPHB4. Our data highlights the pathogenetic importance of this interaction and indicts EPHB4-RAS-ERK signaling pathway as a major cause for CMs and AVMs. Modulating activity of the EPHB4-RAS-ERK pathway would be a novel therapeutic strategy.

Downloaded from http://circ.ahajournals.org/ by guest on July 8, 2017

Circulation

Authors

Mustapha Amyere, PhD[1]*; Nicole Revencu, MD, PhD[2]*; Raphaël Helaers, PhD[1]; Eleonore Pairet, BSC[3]; Eulalia Baselga, MD[4]; Maria R. Cordisco, MD[5,6]; Wendy Chung, MD, PhD[7]; Josée Dubois, MD[8];Jean-Philippe Lacour, MD[9]; Loreto Martorell, MD[10]; Juliette Mazereeuw-Hautier, MD, PhD[11]; Reed E. Pyeritz, MD, PhD[12]; David J. Amor, MD[13]; Annouk Bisdorff, MD[14]; Francine Blei, MD[15]; Hannah Bombei, MSc[16]; Anne Dompmartin, MD, PhD[17], David Brooks, MD[18]; Juliette Dupont, MD[19]; Maria Antonia González-Enseñat, MD[20]; Ilona Frieden, MD[21]; Marion Gérard, MD[22]; Malin Kvarnung, MD[23]; Andrea Kwan Hanson-Kahn, MSc[24]; Louanne Hudgins, MD[25]; Christine Léauté-Labrèze, MD[26]; Catherine McCuaig, MD[27]; Denise Metry, MD[28]; Philippe Parent, MD[29]; Carle Paul, MD, PhD[30]; Florence Petit, MD[31]; Alice Phan, MD[32];

Isabelle Quéré, MD[33]; Aicha Salhi, MD[34]; Anne Turner, MD[35]; Pierre Vabres, MD[36]; Asuncion Vicente, MD[37]; Orli Wargon, MD[38] ; Shoji Watanabe, MD, PhD[39]; Lisa Weibel, MD[40]; Ashley Wilson, MSc[41]; Marcia Willing, MD[42]; John B. Mulliken, MD[43];

Laurence M. Boon, MD, PhD[1,44]; Miikka Vikkula, MD, PhD[1]

*These authors contributed equally to this work

Author Contributions

M.A. designed the experiments, performed SNP array experiments, linkage analysis, and whole exome sequencing experiments and targeted sequencing. He analyzed the NGS data, performed the functional studies and drafted the manuscript. N.R. performed clinical phenotyping, collection of samples and drafted the clinical part of the manuscript. R.H. provided bioinformatics support for the use "Highlander". E.P. helped in analysis of clinical data. (E.B.; M.C.; W.C.; J.D.; J-P.L.; L.M.; J.M.; R.P.; D.A.; A.B.; F.B.; H.B.; A.D.; D.B.; J.D.; M.E.; I.F.; M.G.; M.K.; A.K.; L.H.; C.L.; Mc.C.; D.M.; P.P.; C.P.; F.P.; A.P.; I.Q.; A.S.; A.T.; O.W.; P.V.; A.V.; S.W.; L.W.; A.W.; M.W.; J.B.M. and L.M.B) provided clinical expertise, clinical data, patient recruitment and collection of samples. M.V. initiated and supervised the study. L.M.B., J.B.M. and M.V. developed the manuscript.

Downloaded from http://circ.ahajournals.org/ by guest on July 8, 2017

Acknowledgements

We are grateful to all the patients and their family members who participated in this study. We thank the Fondation Belge contre le Cancer and the Genetics Platform of Université catholique de Louvain for access to the Next Generation Sequencers. The authors also thank Audrey Debue for help in NGS experiments, Laetitia De Roeck for help in Sanger sequencing, Lieven Desmet for help in statistical analysis and Ms Liliana Niculescu for secretarial help.

Sources of Funding

These studies were partially supported by funding from the de Duve Institute; the Belgian Science Policy Office Interuniversity Attraction Poles (BELSPO-IAP) program through the project IAP P7/43- Belgian Medical Genomics Initiative (BeMGI); the Fonds de la Recherche Scientifique - FNRS under Grant n° T.0026.14 (to M.V.), and n° T.0146.16 (to L.M.B.).

Disclosures

None

Downloaded from http://circ.ahajournals.org/ by guest on July 8, 2017

Affiliations

[1]Human Molecular Genetics, de Duve Institute, Université Catholique de Louvain, Brussels, Belgium; [2]Center for Human Genetics, Cliniques Universitaires St Luc, Université Catholique de Louvain, Brussels, Belgium; [3]Université Catholique de Louvain, Brussels, Belgium; [4]Department of Dermatology, Hospital de la Santa Creu I Sant Pau, Barcelona, Spain; [5]Department of Dermatology, Hospital Garrahan, Buenos Aires, Argentina; [6]Strong Hospital, University of Rochester School of Medicine and Dentistry, Rochester, NY; [7]Departments of Pediatrics and Medicine, Columbia University, New York, NY; [8]Department of Medical Imaging, Sainte-Justine Mother-Child University Hospital, Montreal, Canada; [9]Service de Dermatologie, Centre Hospitalo-Universitaire de Nice, Nice, France ; [10]Genética Molecular, Hospital Sant Joan de Déu, Barcelona, Spain; [11]Service de Dermatologie, Centre de Référence des Maladies Rares de la Peau, Hôpital Larrey, Toulouse, France;[12]Departments of Medicine and Genetics, Perelman School of Medicine at the University of Pennsylvania, Philadelphia, PA; [13]Victorian Clinical Genetics Services, Murdoch Children's Research Institute, Royal Children's

Hospital, Parkville, Victoria, Australia; [14]Departments of Pediatrics and Medicine, Columbia University, New York, NY & Department of Neuroradiology, Lariboisière Hospital, Paris, France; [15]Vascular Anomalies Program, Lenox Hill Hospital, New York, NY & Vascular Birthmark Institute of New York, Roosevelt Hospital, New York, NY; [16]Department of Pediatrics- Medical Genetics University of Iowa Carver College of Medicine, Iowa City, IA; [17]Department of Dermatology, Université de Caen Basse Normandie, CHU Caen, Caen, France; [18]Department of Urology, Wake Forest School of Medicine, Winston Salem, NC; [19]Genetics Service, Pediatric Department, University Hospital Santa Maria, Lisbon, Portugal; [20]Department of Dermatology, Hospital Sant Joan de Deu, Barcelona, Spain; [21]Department of Dermatology, School of Medicine, University of California, San Francisco, San Francisco, CA; [22]Department of Genetics, University Hospital, Caen, France; [23]Department of Molecular Medicine and Surgery, Center for Molecular Medicine, Karolinska Institutet, Stockholm, Sweden; [24]Department of Pediatrics, Division of Medical Genetics, Stanford University School of Medicine, Stanford, CA; [25]Department of Pediatrics, Division of Medical Genetics, Stanford University School of Medicine, Stanford, CA; [26]Hôpital Pellegrin Enfants, Bordeaux, France; [27]Hôpital Sainte-Justine, Montréal, QC, Canada; [28]Department of Dermatology, Texas Children's Hospital, Houston, TX; [29]Département de Pédiatrie et Génétique Médicale, CHRU Hôpital Morvan, Brest, France; [30]Department of Dermatology, Paul Sabatier University, Toulouse, France; [31]Service de Génétique Clinique, Hôpital Jeanne de Flandre, CHRU Lille, France; [32]Pediatric Dermatology Unit, Claude Bernard-Lyon, University and Hospices Civils de Lyon, Hôpital Femme-Mère-Enfant, Lyon, France; [33]Centre Hospitalier Universitaire, Montpellier, France; [34]Dermatolgie, Faculté de Médecine d'Alger, Alger, Algeria; [35]Department of Medical Genetics, Sydney Children's Hospital, Randwick, New South Wales, Australia; [36]Service de

Downloaded from http://circ.ahajournals.org/ by guest on July 8, 2017

Dermatologie, Centre Hospitalo-Universitaire Dijon-Bourgogne, Dijon, France; [37]Department of Dermatology, Hospital Sant Joan de Deu, Barcelona, Spain; [38]Department of Pediatric Dermatology, Sydney Children's Hospital: School of Women's & Children's Health University of New South Wales, Sydney, New South Wales, Australia; [39]Department of Plastic and Reconstructive Surgery, University of Tokyo, Tokyo, Japan; [40]Department of Pediatric Dermatology, University Children's Hospital Zurich, Zurich, Switzerland; [41]Children's Hospital of New York, New York, NY; [42]University of Iowa Hospitals and Clinics, Iowa City, IA & Department of Pediatrics, Washington University, St. Louis, MI; [43]Vascular Anomalies Center, Boston Children's Hospital and Harvard Medical School, Boston, MA; [44]Center for Vascular Anomalies, Division of Plastic Surgery, Cliniques Universitaires Saint-Luc, Brussels, Belgium

Downloaded from http://circ.ahajournals.org/ by guest on July 8, 2017

Disclosures

The authors declare no conflict of interest and no competing financial interest.

Web Resources

The URLs for data presented herein are as follows:

1000 Genomes, http://www.1000genomes.org/

BWA: bio-bwa.sourceforge.net/

COSMIC, http://cancer.sanger.ac.uk/cosmic

ExAC Browser, http://exac.broadinstitute.org/

Exome Aggregation Consortium(ExAC), http://exac.broadinstitute.org/

Functional Analysis though Hidden Markov Models (FATHMM),http://fathmm.biocompute.org.uk/

Genome of the Netherlands (GoNL), http://www.nlgenome.nl/

Highlander, http://sites.uclouvain.be/highlander/

Human Genome Variation Society, http://www.hgvs.org/mutnomen/

Mutation Assessor, http://mutationassessor.org/

Mutation Taster, http://www.mutationtaster.org/

NextGene: http://www.softgenetics.com/

NHLBI Exome Sequencing Project (ESP), http://evs.gs.washington.edu/EVS/

Online Mendelian Inheritance in Man (OMIM), http://www.omim.org

Picard: broadinstitute.github.io/picard/

Polyphen2, http://genetics.bwh.harvard.edu/pph2/

SIFT, http://sift.jcvi.org/

Downloaded from http://circ.ahajournals.org/ by guest on July 8, 2017

References

1. Mulliken JB YA. Vascular birthmarks: hemangiomas and malformations. *WB Saunders, Philadelphia*. 1988.
2. Gross BA and Du R. Natural history of cerebral arteriovenous malformations: a meta-analysis. *J Neurosurg*. 2013;118:437-443.
3. McDonald J, Bayrak-Toydemir P and Pyeritz RE. Hereditary hemorrhagic telangiectasia: an overview of diagnosis, management, and pathogenesis. *Genet Med* 2011;13:607-616.
4. Fleetwood IG and Steinberg GK. Arteriovenous malformations. *Lancet*. 2002;359:863-873.
5. Sturge WA. On Hemianaesthesia of Special and General Sensation. *Br Med J*. 1878;1:783-785.
6. Kohout MP, Hansen M, Pribaz JJ and Mulliken JB. Arteriovenous malformations of the head and neck: natural history and management. *Plast Reconstr Surg*. 1998;102:643-654.
7. Shovlin CL. Hereditary haemorrhagic telangiectasia: pathophysiology, diagnosis and treatment. *Blood Rev*. 2010;24:203-219.
8. Eerola I, Boon LM, Mulliken JB, Burrows PE, Dompmartin A, Watanabe S, Vanwijck R and Vikkula M. Capillary malformation-arteriovenous malformation, a new clinical and genetic disorder caused by RASA1 mutations. *Am J Hum Genet*. 2003;73:1240-1249.
9. Revencu N, Boon LM, Mulliken JB, Enjolras O, Cordisco MR, Burrows PE, Clapuyt P, Hammer F, Dubois J, Baselga E, Brancati F, Carder R, Quintal JM, Dallapiccola B, Fischer G, Frieden IJ, Garzon M, Harper J, Johnson-Patel J, Labreze C, Martorell L, Paltiel HJ, Pohl A, Prendiville J, Quere I, Siegel DH, Valente EM, Van Hagen A, Van Hest L, Vaux KK, Vicente A, Weibel L, Chitayat D and Vikkula M. Parkes Weber syndrome, vein of Galen aneurysmal

malformation, and other fast-flow vascular anomalies are caused by RASA1 mutations. *Hum Mutat*. 2008;29:959-965.
10. Revencu N, Boon LM, Mendola A, Cordisco MR, Dubois J, Clapuyt P, Hammer F, Amor DJ, Irvine AD, Baselga E, Dompmartin A, Syed S, Martin-Santiago A, Ades L, Collins F, Smith J, Sandaradura S, Barrio VR, Burrows PE, Blei F, Cozzolino M, Brunetti-Pierri N, Vicente A, Abramowicz M, Desir J, Vilain C, Chung WK, Wilson A, Gardiner CA, Dwight Y, Lord DJ, Fishman L, Cytrynbaum C, Chamlin S, Ghali F, Gilaberte Y, Joss S, Boente Mdel C, Leaute-Labreze C, Delrue MA, Bayliss S, Martorell L, Gonzalez-Ensenat MA, Mazereeuw-Hautier J, O'Donnell B, Bessis D, Pyeritz RE, Salhi A, Tan OT, Wargon O, Mulliken JB and Vikkula M. RASA1 mutations and associated phenotypes in 68 families with capillary malformation-arteriovenous malformation. *Hum Mutat*. 2013;34:1632-1641.
11. Boon LM, Mulliken JB and Vikkula M. RASA1: variable phenotype with capillary and arteriovenous malformations. *Curr Opin Genet Dev*. 2005;15:265-269.
12. Thiex R, Mulliken JB, Revencu N, Boon LM, Burrows PE, Cordisco M, Dwight Y, Smith ER, Vikkula M and Orbach DB. A novel association between RASA1 mutations and spinal arteriovenous anomalies. *Format: AbstractSend to*
AJNR Am J Neuroradiol. 2010;31:775-779.
13. Henkemeyer M, Rossi DJ, Holmyard DP, Puri MC, Mbamalu G, Harpal K, Shih TS, Jacks T and Pawson T. Vascular system defects and neuronal apoptosis in mice lacking ras GTPase-activating protein. *Nature*. 1995;377:695-701.
14. Burrows PE, Gonzalez-Garay ML, Rasmussen JC, Aldrich MB, Guilliod R, Maus EA, Fife CE, Kwon S, Lapinski PE, King PD and Sevick-Muraca EM. Lymphatic abnormalities are associated with RASA1 gene mutations in mouse and man. *Proc Natl Acad Sci U S A*. 2013;110:8621-8626.
15. Dong C, Wei P, Jian X, Gibbs R, Boerwinkle E, Wang K and Liu X. Comparison and integration of deleteriousness prediction methods for nonsynonymous SNVs in whole exome sequencing studies. *Hum Mol Genet*. 2015;24:2125-2137.
16. Lek M, Karczewski KJ, Minikel EV, Samocha KE, Banks E, Fennell T, O'Donnell-Luria AH, Ware JS, Hill AJ, Cummings BB, Tukiainen T, Birnbaum DP, Kosmicki JA, Duncan LE, Estrada K, Zhao F, Zou J, Pierce-Hoffman E, Berghout J, Cooper DN, Deflaux N, DePristo M, Do R, Flannick J, Fromer M, Gauthier L, Goldstein J, Gupta N, Howrigan D, Kiezun A, Kurki MI, Moonshine AL, Natarajan P, Orozco L, Peloso GM, Poplin R, Rivas MA, Ruano-Rubio V, Rose SA, Ruderfer DM, Shakir K, Stenson PD, Stevens C, Thomas BP, Tiao G, Tusie-Luna MT, Weisburd B, Won HH, Yu D, Altshuler DM, Ardissino D, Boehnke M, Danesh J, Donnelly S, Elosua R, Florez JC, Gabriel SB, Getz G, Glatt SJ, Hultman CM, Kathiresan S, Laakso M, McCarroll S, McCarthy MI, McGovern D, McPherson R, Neale BM, Palotie A, Purcell SM, Saleheen D, Scharf JM, Sklar P, Sullivan PF, Tuomilehto J, Tsuang MT, Watkins HC, Wilson JG, Daly MJ, MacArthur DG and Exome Aggregation C. Analysis of protein-coding genetic variation in 60,706 humans. *Nature*. 2016;536:285-291.
17. Newcombe RG. Interval estimation for the difference between independent proportions: comparison of eleven methods. *Stat Med*. 1998;17:873-890.
18. MacArthur DG, Manolio TA, Dimmock DP, Rehm HL, Shendure J, Abecasis GR, Adams DR, Altman RB, Antonarakis SE, Ashley EA, Barrett JC, Biesecker LG, Conrad DF, Cooper GM, Cox NJ, Daly MJ, Gerstein MB, Goldstein DB, Hirschhorn JN, Leal SM, Pennacchio LA, Stamatoyannopoulos JA, Sunyaev SR, Valle D, Voight BF, Winckler W and

Downloaded from http://circ.ahajournals.org/ by guest on July 8, 2017

Gunter C. Guidelines for investigating causality of sequence variants in human disease. *Nature*. 2014;508:469-476.
19. Chrencik JE, Brooun A, Kraus ML, Recht MI, Kolatkar AR, Han GW, Seifert JM, Widmer H, Auer M and Kuhn P. Structural and biophysical characterization of the EphB4*ephrinB2 protein-protein interaction and receptor specificity. *J Biol Chem.* 2006;281:28185-28192.
20. Molho-Pessach V, Agha Z, Libster D, Lerer I, Burger A, Jaber S, Abeliovich D and Zlotogorski A. Evidence for clinical and genetic heterogeneity in hereditary benign telangiectasia. *J Am Acad Dermatol.* 2007;57:814-818.
21. Bayrak-Toydemir P, McDonald J, Akarsu N, Toydemir RM, Calderon F, Tuncali T, Tang W, Miller F and Mao R. A fourth locus for hereditary hemorrhagic telangiectasia maps to chromosome 7. *Am J Med Genet A.* 2006;140:2155-2162.
22. Cole SG, Begbie ME, Wallace GM and Shovlin CL. A new locus for hereditary haemorrhagic telangiectasia (HHT3) maps to chromosome 5. *J Med Genet*. 2005;42:577-582.
23. Gold MH, Eramo L and Prendiville JS. Hereditary benign telangiectasia. *Pediatr Dermatol.* 1989;6:194-197.
24. Ryan TJ and Wells RS. Hereditary benign telangiectasia. *Trans St Johns Hosp Dermatol Soc.* 1971;57:148-156.
25. Wells RS and Dowling GB. Hereditary benign telangiectasia. *Br J Dermatol.* 1971;84:93-94.
26. Parambil JG. Hereditary Hemorrhagic Telangiectasia. *Clin Chest Med.* 2016;37:513-521.
27. Limaye N, Wouters V, Uebelhoer M, Tuominen M, Wirkkala R, Mulliken JB, Eklund L, Boon LM and Vikkula M. Somatic mutations in angiopoietin receptor gene TEK cause solitary and multiple sporadic venous malformations. *Nat Genet.* 2009;41:118-124.
28. Amyere M, Aerts V, Brouillard P, McIntyre BA, Duhoux FP, Wassef M, Enjolras O, Mulliken JB, Devuyst O, Antoine-Poirel H, Boon LM and Vikkula M. Somatic uniparental isodisomy explains multifocality of glomuvenous malformations. *Am J Hum Genet.* 2013;92:188-196.
29. Macmurdo CF, Wooderchak-Donahue W, Bayrak-Toydemir P, Le J, Wallenstein MB, Milla C, Teng JM, Bernstein JA and Stevenson DA. RASA1 somatic mutation and variable expressivity in capillary malformation/arteriovenous malformation (CM/AVM) syndrome. *Am J Med Genet A.* 2016;170:1450-1454.
30. Adams RH, Wilkinson GA, Weiss C, Diella F, Gale NW, Deutsch U, Risau W and Klein R. Roles of ephrinB ligands and EphB receptors in cardiovascular development: demarcation of arterial/venous domains, vascular morphogenesis, and sprouting angiogenesis. *Genes Dev.* 1999;13:295-306.
31. Wang HU, Chen ZF and Anderson DJ. Molecular distinction and angiogenic interaction between embryonic arteries and veins revealed by ephrin-B2 and its receptor Eph-B4. *Cell*. 1998;93:741-753.
32. Bai J, Wang YJ, Liu L and Zhao YL. Ephrin B2 and EphB4 selectively mark arterial and venous vessels in cerebral arteriovenous malformation. *J Int Med Res.* 2014;42:405-415.
33. Lin FJ, Tsai MJ and Tsai SY. Artery and vein formation: a tug of war between different forces. *EMBO reports*. 2007;8:920-924.
34. Kaenel P, Hahnewald S, Wotzkow C, Strange R and Andres AC. Overexpression of EphB4 in the mammary epithelium shifts the differentiation pathway of progenitor cells and promotes branching activity and vascularization. *Dev Growth Differ.* 2014;56:255-275.

Downloaded from http://circ.ahajournals.org/ by guest on July 8, 2017

35. Gerety SS, Wang HU, Chen ZF and Anderson DJ. Symmetrical mutant phenotypes of the receptor EphB4 and its specific transmembrane ligand ephrin-B2 in cardiovascular development. *Mol Cell.* 1999;4:403-414.
36. Xiao Z, Carrasco R, Kinneer K, Sabol D, Jallal B, Coats S and Tice DA. EphB4 promotes or suppresses Ras/MEK/ERK pathway in a context-dependent manner: Implications for EphB4 as a cancer target. *Cancer Biol Ther.* 2012;13:630-637.
37. Kawasaki J, Aegerter S, Fevurly RD, Mammoto A, Mammoto T, Sahin M, Mably JD, Fishman SJ and Chan J. RASA1 functions in EPHB4 signaling pathway to suppress endothelial mTORC1 activity. *J Clin Invest.* 2014;124:2774-2784.
38. Holland SJ, Gale NW, Gish GD, Roth RA, Songyang Z, Cantley LC, Henkemeyer M, Yancopoulos GD and Pawson T. Juxtamembrane tyrosine residues couple the Eph family receptor EphB2/Nuk to specific SH2 domain proteins in neuronal cells. *EMBO J.* 1997;16:3877-3888.
39. Shirley MD, Tang H, Gallione CJ, Baugher JD, Frelin LP, Cohen B, North PE, Marchuk DA, Comi AM and Pevsner J. Sturge-Weber syndrome and port-wine stains caused by somatic mutation in GNAQ. *N Engl J Med.* 2013;368:1971-1979.
40. Thomas AC, Zeng Z, Riviere JB, O'Shaughnessy R, Al-Olabi L, St-Onge J, Atherton DJ, Aubert H, Bagazgoitia L, Barbarot S, Bourrat E, Chiaverini C, Chong WK, Duffourd Y, Glover M, Groesser L, Hadj-Rabia S, Hamm H, Happle R, Mushtaq I, Lacour JP, Waelchli R, Wobser M, Vabres P, Patton EE and Kinsler VA. Mosaic Activating Mutations in GNA11 and GNAQ Are Associated with Phakomatosis Pigmentovascularis and Extensive Dermal Melanocytosis. *J Invest Dermatol.* 2016;136:770-778.
41. Couto JA, Huang AY, Konczyk DJ, Goss JA, Fishman SJ, Mulliken JB, Warman ML and Greene AK. Somatic MAP2K1 Mutations Are Associated with Extracranial Arteriovenous Malformation. *Am J Hum Genet.* 2017;100:546-554.
42. Mohr JP, Parides MK, Stapf C, Moquete E, Moy CS, Overbey JR, Al-Shahi Salman R, Vicaut E, Young WL, Houdart E, Cordonnier C, Stefani MA, Hartmann A, von Kummer R, Biondi A, Berkefeld J, Klijn CJ, Harkness K, Libman R, Barreau X, Moskowitz AJ and international Ai. Medical management with or without interventional therapy for unruptured brain arteriovenous malformations (ARUBA): a multicentre, non-blinded, randomised trial. *Lancet*. 2014;383:614-621.
43. Liu AS, Mulliken JB, Zurakowski D, Fishman SJ and Greene AK. Extracranial arteriovenous malformations: natural progression and recurrence after treatment. *Plast Reconstr Surg.* 2010;125:1185-1194.

Downloaded from http://circ.ahajournals.org/ by guest on July 8, 2017

Downloaded from http://circ.ahajournals.org/ by guest on July 8, 2017

Table 1. 54 families with EPHB4 mutations and corresponding clinical features

D of screened patient	hgvs DNA	hgvs protein	Consensus prediction	Number of mutation carriers	Number of patients with CM	Location of AVM	Location of Parkes Weber Syndrome	ExAC allele frequency
CM-13-HO-II-6A	c.33delG	p.L12Wfs*10	40	7	7	0	0	
CM-565-10	c.123+3G>C; r.123_411del	p.W18Vfs*16	20	4	3	0	0	
CM-415-10	c.175G>A	p.E59K	4	1	1	0	left arm	
CM-184-10	c.221G>C	p.R74P	4	2	2	0	0	
CM-177-10	c.389G>A	p.W130*	42	1(‡)	1	0	0	
CM-219-10	c.412-1G>T		33	4	3	0	0	
CM-378-10	c.447_448insGAAG	p.R150Efs*74	40	3	2	0	0	
CM-348-10	c.481_485delGTCAAinsTT	p.V161_K162delinsL	10	1 (†)	1	0	0	
CM-115-100	c.560T>C	p.L187P	5	1	1	0	left leg	
CM-291-10	c.632_633delTG	p.V211Afs*11	40	2	2	0	0	
CM-568-10	c.730C>T	p.Q244*	43	3	3	0	0	
CM-90-10	c.802T>C	p.C268R	6	4	4	0	right leg	
I-302-10	c.345_347delCTA	p.Y115del	10	1	1	right face	0	
CM-455-10	c.1054C>T	p.R352*	42	1 (‡)	1	0	0	
CM-558-10	c.1054C>T	p.R352*	42	2	2	0	0	
CM-546-2	c.1077_1081delCCGCT	p.L359fs*19	40	2	2	0	0	
CM-337-106	c.1123G>T	p.Gly375*	41	3	3	0	0	
CM-345-10	c.1177_1177delG	p.V393Ffs*17	40	1	1	0	0	
CM-391-100	c.1291C>T	p.R431*	42	3	3	0	0	0.00001
CM-377-10	c.1406T>G	p.V469G	5	4	4	0	0	
CM-120-10	c.1423-6G>A; r.1422_1423insACAG	p.G475Tfs*39	22	4	3	0	0	
CM-147-100	c.1546G>A	p.G516R	5	2	1	left face and lip	0	0.00002
CM-162-100	c.1546G>A	p.G516R	5	1	1	left face	0	
CM-538-10	c.1546G>A	p.G516R	5	2	2	0	0	
CM-487-10	c.1558C>T	p.Gln520*	41	1	1	0	0	
CM-544-10	c.1558C>T	p.Gln520*	41	1	1	0	0	
CM-470-10	c.1588+5G>C		22	1(†)	1	0	right arm	
CM-323-10	c.1615delG	p.A539fs*2	40	3	3	0	right leg	
CM-131-101	c.1692-1G>A		33	1 (†)	1	0	0	
CM-401-10	c.1733_1734insA	p.G579Rfs*10	40	2	2	0	0	
CM-224-11	c.1788T>G	p.Y596*	42	2	2	0	left arm	

Downloaded from http://circ.ahajournals.org/ by guest on July 8, 2017

CM-239-10	**c.1870+2T>C**		**33**	**2**	**1**	**left face**	**0**	
CM-298-10	**c.1966C>T**	**p.R656W**	**5**	**1**	**1**	**0**	**0**	
CM-397-10	**c.1990G>A**	**p.E664K**	**6**	**4**	**3**	**VGAM/VGAM**	**0**	
CM-105-11	**c.2037_2038insT**	**p.E680***	**40**	**2**	**2**	**left arm**	**right leg**	
CM-340-10	**c.2173G>A**	**p.A725T**	**6**	**1 (†)**	**1**	**0**	**0**	
CM-459-10-1	**c.2215C>T**	**p.R739***	**41**	**2**	**2**	**0**	**0**	**0.00002**
CM-74-II-1	**c.2215C>T**	**p.R739***	**41**	**1**	**1**	**0**	**0**	**0.00002**
CM-297-2	**c.2233A>G**	**p.N745D**	**6**	**1 (†)**	**1**	**0**	**0**	
CM-433-11	**c.2233A>G**	**p.N745D**	**6**	**4**	**4**	**0**	**right arm**	
CM-236-10	**c.2365C>T**	**p.P789S**	**6**	**2**	**1**	**left face**	**0**	
CM-324-10	**c.2366C>G**	**p.P789R**	**6**	**2**	**2**	**0**	**0**	
CM-488-10	**c.2379delC**	**p.A793fs*16**	**40**	**1**	**1**	**0**	**0**	
CM-498-10	**c.2418C>G**	**p.Y806***	**42**	**3**	**3**	**0**	**0**	
CM-373-10	**c.2419G>A**	**p.G807R**	**6**	**2**	**2**	**left ear**	**0**	
CM-407-2	**c.2458C>A**	**p.P820T**	**6**	**2**	**2**	**0**	**0**	
CM-567-10	**c.2459C>T**	**p.P820L**	**6**	**3**	**3**	**lips**	**0**	
CM-490-10	**c.2484+1G>A**		**33**	**1**	**1**	**D8-L1 perimedullar AVF**	**0**	
CM-444-10	**c.2512C>T**	**p.R838W**	**6**	**1**	**1**	**0**	**0**	**0.00001**
CM-282-10	**c.2533T>C**	**p.C845R**	**6**	**1**	**1**	**face and upper lip**	**0**	
CM-426-10	**c.2567G>A**	**p.C856Y**	**6**	**1 (‡)**	**1**	**0**	**0**	
CM-110-101	**c.2590C>T**	**p.R864W**	**6**	**1 (†)**	**1**	**0**	**0**	
CM-390-10	**c.2590C>T**	**p.R864W**	**6**	**2**	**2**	**0**	**0**	
CM-157-10	**c.2621T>C**	**p.L874P**	**6**	**1 (†)**	**1**	**left face**	**0**	

hgvs = Annotation based on Human Genome Variation Society; Consensus prediction = Functional predictions retrieved from dbNSFP4.1 (damaging in SIFT, deleterious in LRT, high or medium in Mutation Assessor, damaging in Fathmm, disease-causing in Mutation Taster, and a score > 0.5 in Polyphen2); ExAC = Exome Aggregation Consortium.

Consensus prediction column gives the number of different algorithms that suggest a variant to be damaging. The maximum is 6 for missense variants, as six different algorithms are used (Sift, LRT, Mutation Assessor, FATHMM, Mutation Taster and Polyphen2). In addition, if the variant affects splicing (evaluated by two distinct algorithms: ada and rf), +1 or +2 is added. Furthermore, to better distinguish variants with high potential for deleterious effects, +10 is added for variants that cause a loss of a start or stop-codon, or insertion or deletion of a codon with or without codon change. +20 is added for variants in splice site regions, and +30 for variants in consensus splice sites and for small exon deletions. +40 is added for variants causing a frame shift or appearance of a premature STOP codon.

VGAM : vein of Galen aneurysmal malformation; VGAM/VGAM : 2 affected individuals in the same family; (*) Non-sense mutation position in protein. (†) : DNA not available from other affected family members ; (‡) : confirmed sporadic case.

Figure Legends

Figure 1. Schematic representation of *EPHB4* gene and its protein-coding domains, with CM-AVM2-causing mutations. EPHB4 domains: Ephrin-b2 binding domain; cysteine-rich domain, two fibronectin (FN) type III domains; transmembrane (TM) region; tyrosine kinase domain and SAM domain. Mutations: above, causing premature stops, frame-shifts and splice site changes; below: missense substitutions predicted to be damaging. Four expressed mutations marked in red.

Downloaded from http://circ.ahajournals.org/ by guest on July 8, 2017

Figure 2. Missense mutations in EPHB4 from 4 CM-AVM2 patients lead to proteosomal degradation. COS7 cells are transiently transfected with EGFP-EPHB4 wild type EPHB4 or with one of the 4 mutations. Evaluation of ubiquitination in cells pre-treated with chloroquine or MG132 (**A**). Protein expression accessed by Western Blotting using anti-EPHB4, or monoclonal anti-β-actin. Representative experiments of three transfections performed are shown. Confocal laser scanning microscopy of cells transiently expressing wild-type EGFP-EPHB4 **(B)** or the 4 EGFP-EPHB4-mutants **(C-F)**. Images are representative of 100 analyzed cells from 3 independent transfections. Arrow indicates EPHB4 ; NT = non-treated ; scale bars = 5 μm.

Figure 3. Phenotypic spectrum associated with EPHB4 mutations.

Multifocal CMs and Bier spots **(A)**. Multifocal CMs **(B)**. Multifocal CMs with white surrounding halo **(C)**. Multiple telangiectasias on upper thorax **(D)**. Multiple labial and peribuccal telangiectasias **(E)**. Multifocal CMs with geographic borders and pale central zone **(F)**. AVM on the face **(G).** Vein of Galen aneurysmal malformation **(H)**. Parkes Weber

syndrome in right leg **(I)**.

Figure 4. Role of EPHB4 in AVM formation.

Artery-fated angioblasts (cell colored in red) express EphrinB2 and inhibit expression of venous markers (EPHB4, and Chicken ovalbumin upstream promoter transcription factor II, COUP-TFII). Venous fated ECs (cell colored in blue), express COUP-TFII and thereby the EphrinB2 receptor EPHB4, and suppress expression of Notch signaling. EphrinB2/EPHB4 interaction responsible for suppression of RAS/MEK/ERK and RAS/AKT/mTORC1 pathways. Lack of EPHB4 or p120RASGAP in venous endothelial cells of CM-AVM2 and CM-AVM1 patients, respectively (cell colored in light green), results in constitutive activation of RAS/MEK/ERK and RAS/AKT/mTORC1 pathways, leading to abnormal differentiation of ECs and disorganized vascular development.

Downloaded from http://circ.ahajournals.org/ by guest on July 8, 2017

Circulation

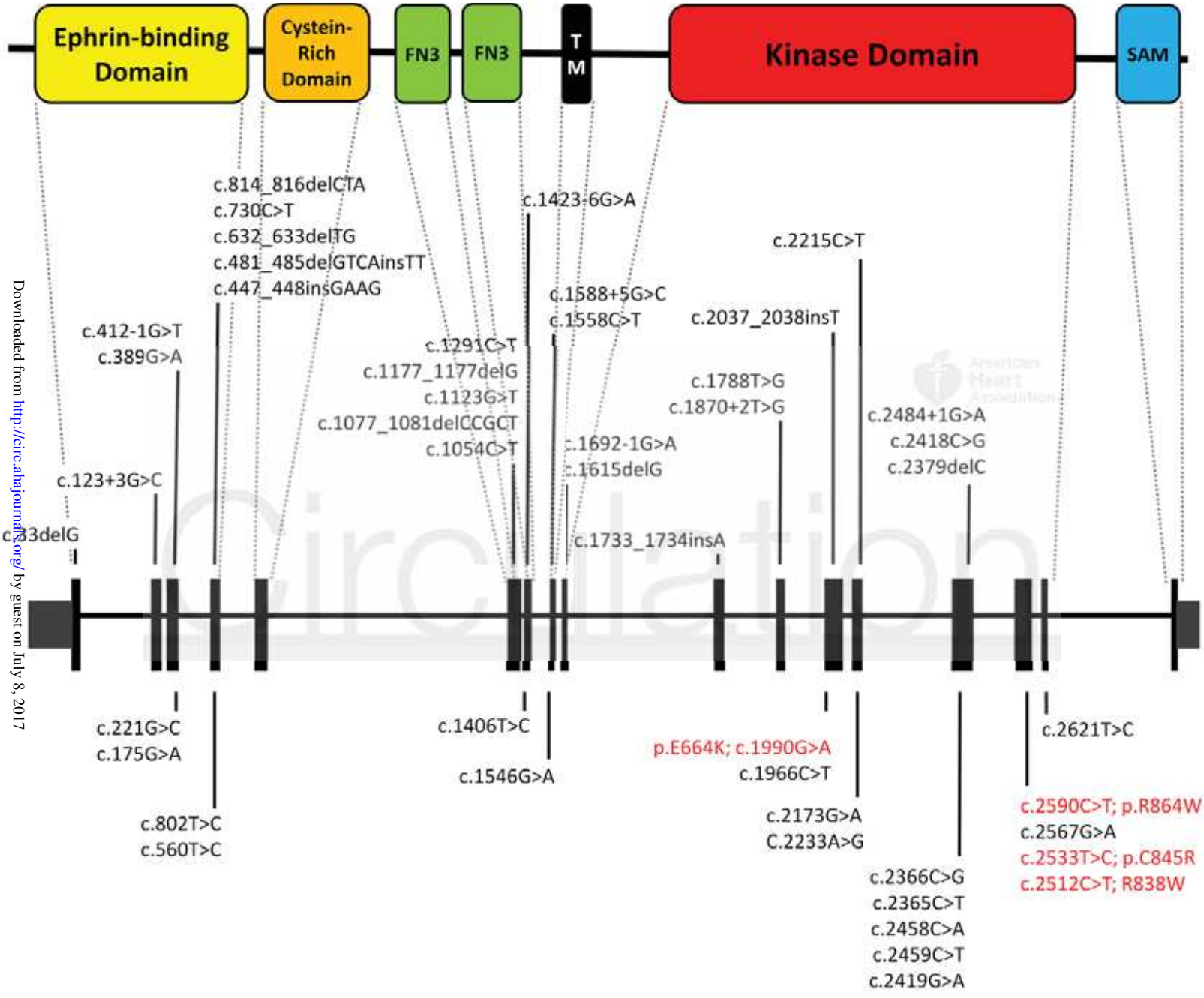

Downloaded from http://circ.ahajournals.org/ by guest on July 8, 2017

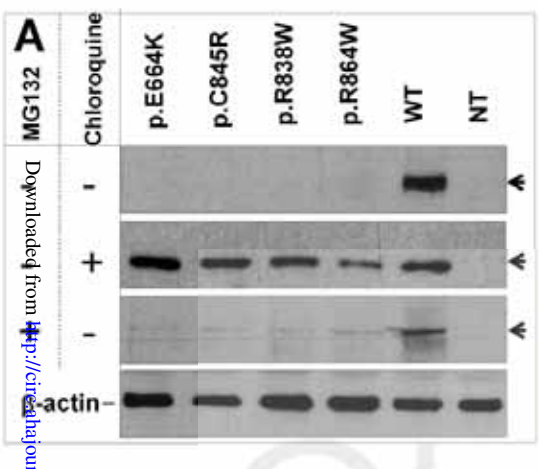

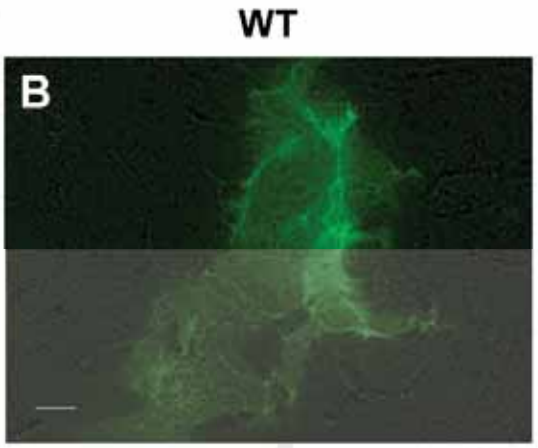

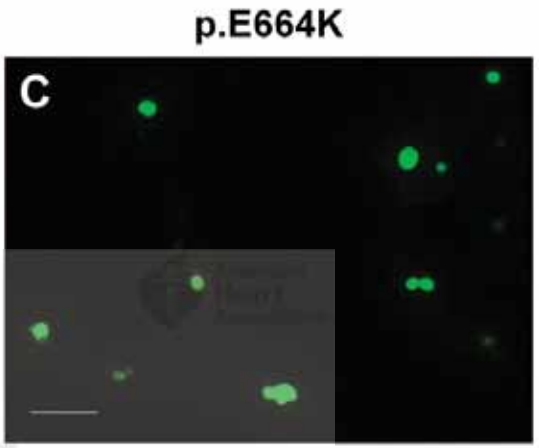

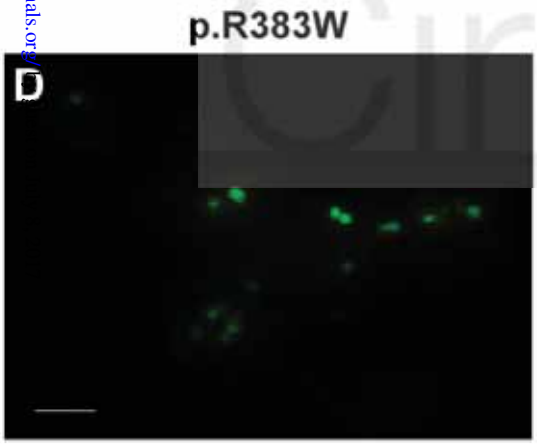

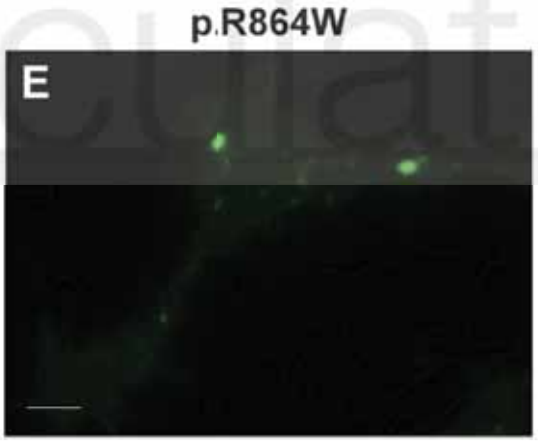

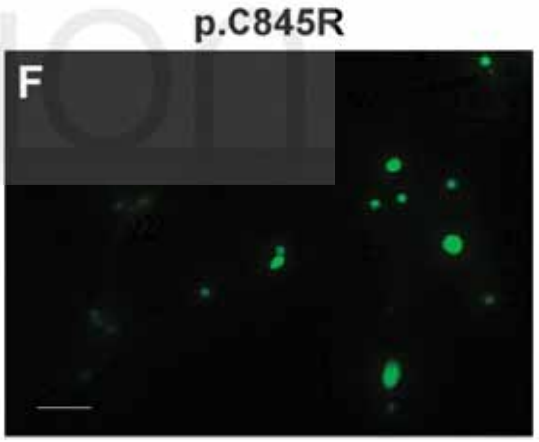

Downloaded from http://circ.ahajournals.org/

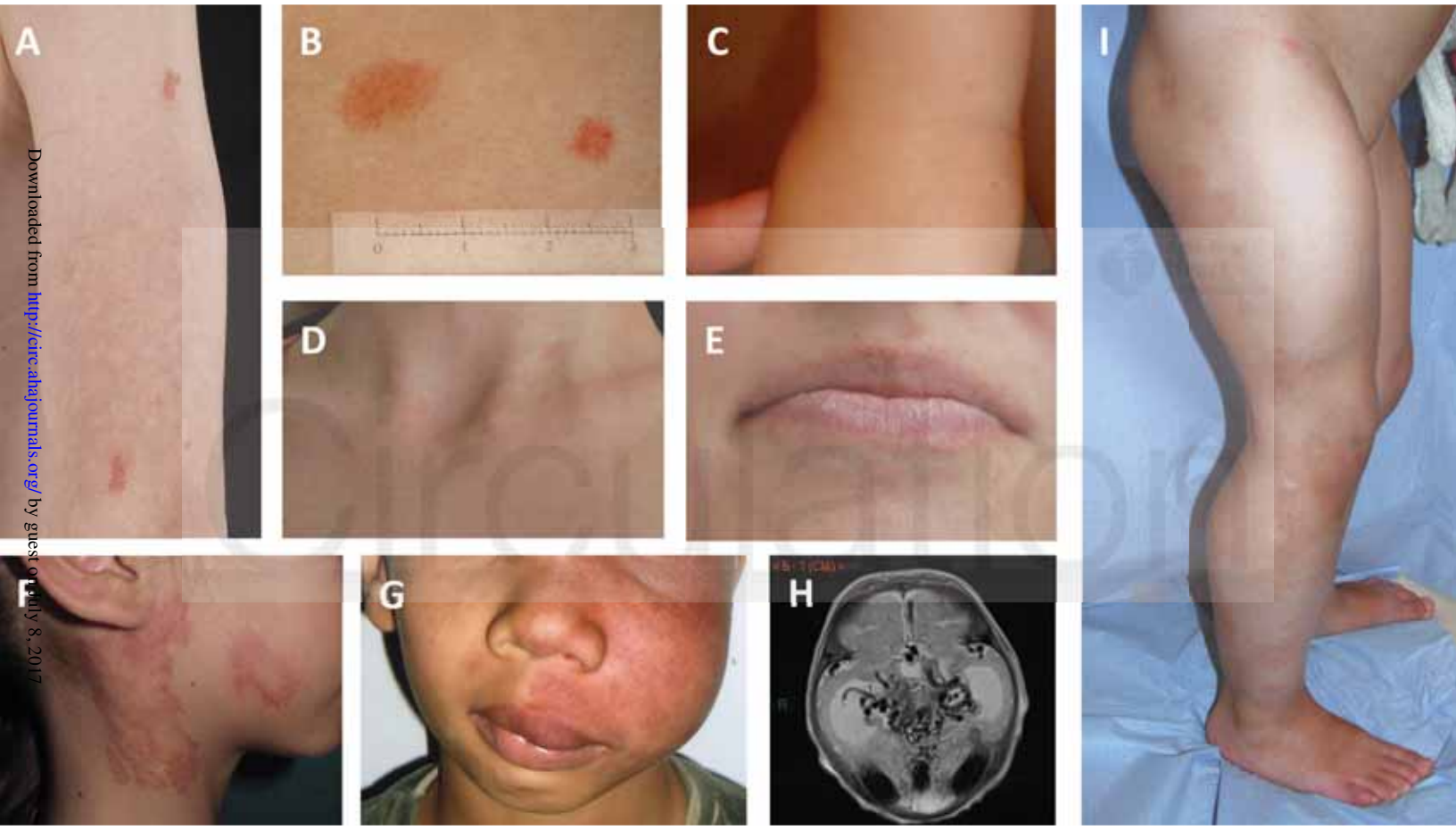

Downloaded from http://circ.ahajournals.org/ by guest on July 8, 2017

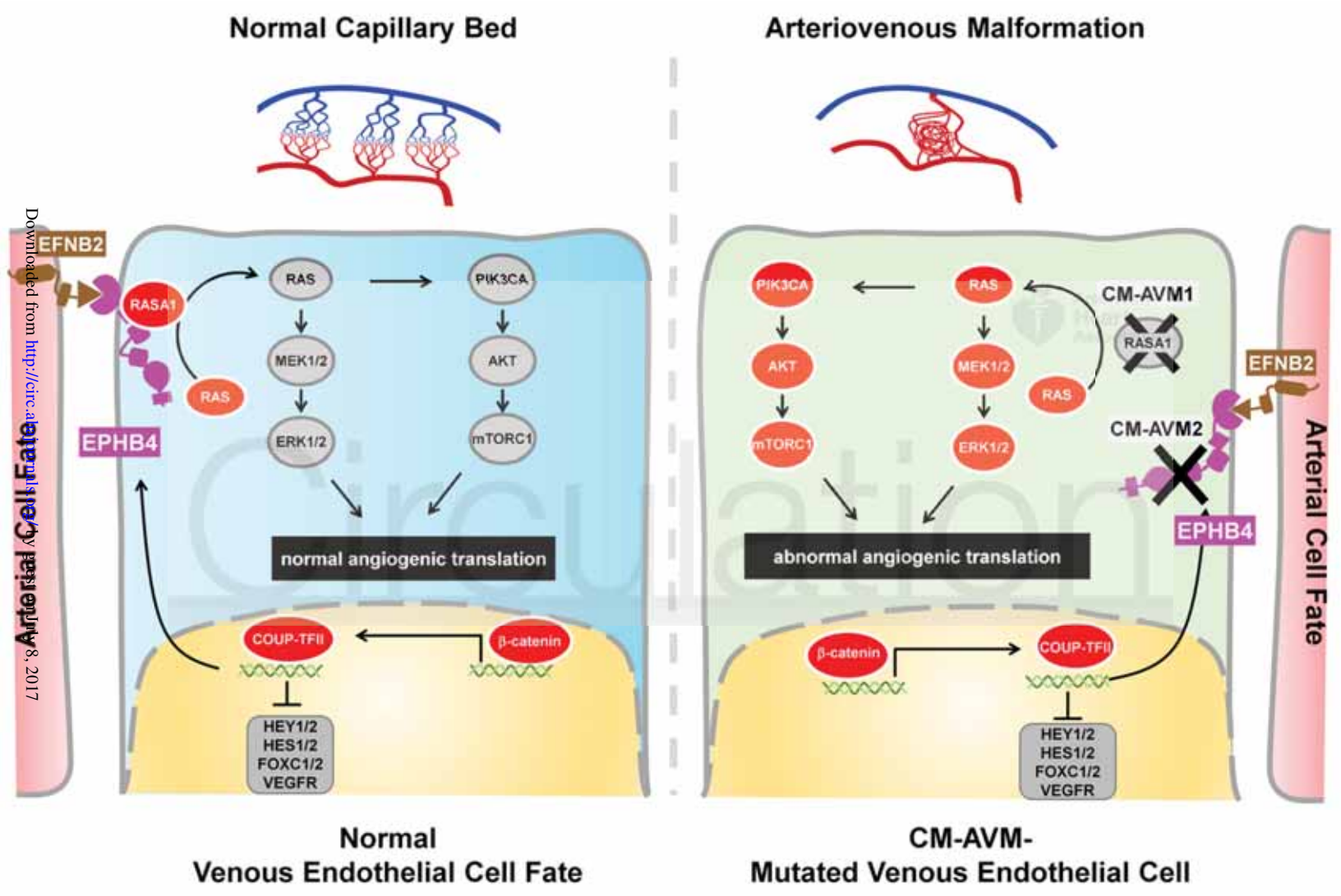

Normal
Venous Endothelial Cell Fate

CM-AVM-
Mutated Venous Endothelial Cell

Downloaded from http://circ.ahajournals.org/ by guest on May 8, 2017

Circulation

American Heart Association®

Germline Loss-of-Function Mutations in EPHB4 Cause a Second Form of Capillary Malformation-Arteriovenous Malformation (CM-AVM2) Deregulating RAS-MAPK Signaling

Mustapha Amyere, Nicole Revencu, Raphaël Helaers, Eleonore Pairet, Eulalia Baselga, Maria R. Cordisco, Wendy K. Chung, Josée Dubois, Jean-Philippe Lacour, Loreto Martorell, Juliette Mazereeuw-Hautier, Reed E. Pyeritz, David J. Amor, Annouk Bisdorff, Francine Blei, Hannah Bombei, Anne Dompmartin, David G. Brooks, Juliette Dupont, Maria A. González-Enseñat, Ilona J. Frieden, Marion Gérard, Malin Kvarnung, Andrea Kwan Hanson-Kahn, Louanne Hudgins, Christine Léauté-Labrèze, Catherine McCuaig, Denise Metry, Philippe Parent, Carle Paul, Florence Petit, Alice Phan, Isabelle Quéré, Aicha Salhi, Anne M. Turner, Pierre Vabres, Asuncion Vicente, Orli Wargon, Shoji Watanabe, Lisa Weibel, Ashley Wilson, Marcia Willing, John B. Mulliken, Laurence M. Boon and Miikka Vikkula

Circulation. published online July 7, 2017;
Circulation is published by the American Heart Association, 7272 Greenville Avenue, Dallas, TX 75231
Copyright © 2017 American Heart Association, Inc. All rights reserved.
Print ISSN: 0009-7322. Online ISSN: 1524-4539

Downloaded from http://circ.ahajournals.org/ by guest on July 8, 2017

The online version of this article, along with updated information and services, is located on the World Wide Web at:
http://circ.ahajournals.org/content/early/2017/07/07/CIRCULATIONAHA.116.026886

Data Supplement (unedited) at:
http://circ.ahajournals.org/content/suppl/2017/07/07/CIRCULATIONAHA.116.026886.DC1

Permissions: Requests for permissions to reproduce figures, tables, or portions of articles originally published in *Circulation* can be obtained via RightsLink, a service of the Copyright Clearance Center, not the Editorial Office. Once the online version of the published article for which permission is being requested is located, click Request Permissions in the middle column of the Web page under Services. Further information about this process is available in the Permissions and Rights Question and Answer document.

Reprints: Information about reprints can be found online at:
http://www.lww.com/reprints

Subscriptions: Information about subscribing to *Circulation* is online at:
http://circ.ahajournals.org//subscriptions/

SUPPLEMENTAL MATERIAL

Table of Contents

MICROARRAY ANALYSIS. Molecular karyotyping was performed on blood DNA of 15 family members of CM-13-HO with Affymetrix Human Mapping 250K *NspI* according to the manufacturer's (Affymetrix) instructions. In brief, total genomic DNA was digested, and fragments were ligated to adaptors and amplified with a single primer. After purification of the PCR products, amplicons were quantified, fragmented, labeled, and hybridized on the array. Signal intensities were measured with Affymetrix GeneChip Scanner 3000 7G. Genotypes were extracted with Affymetrix Genotyping Console software 4.1.4.

EXOME SEQUENCING. Briefly, 1 µg of genomic DNA from 11 blood samples of patients from 9 unrelated families were processed. Exons were captured using the Agilent SureSelect Human All Exon V5 and sequenced with an Illumina HiSeq2000 to generate paired-end, 90-bp reads. Image analysis and base calling were performed by sequence control software real-time analysis and CASAVA software v1.8 (Illumina). Reads were aligned to GRCh37 using software package for mapping Burrows-Wheeler Aligner (BWA; see URLs). Duplicate reads were marked using Picard (see URLs) and excluded from downstream analysis. After merging the BAM files using SAM tools, local realignments around Indels and base quality score recalibration were performed with the Genome Analysis Toolkit (GATK) v2.8. Single-nucleotide variants and small Indels were identified using the GATK Unified Genotyper. Called variants were subsequently annotated, filtered and visualized using Integrative Genome Browser (IGV) and Highlander software; in-house bioinformatics framework (see URLs). We achieved mean coverage of 54-fold, with 82% of target covered at least 20x. We focused on non-synonymous variants (NSVs), splice acceptor and donor-site variants (SSVs), and small insertions/deletions (InDels) that are more likely to be pathogenic than other variants (**supplementary Table 1 and supplementary Table 2**).

TARGETED DEEP-SEQUENCING. A custom AmpliSeq panel was designed (20 amplicons; 6.12 Kb) to sequence all exons and exon-intron boundaries of *RASA1* and *EPHB4* using the Ion PGM™ Sequencer. The whole cohort of 365 index patients was screened. Library enrichment of target region was amplified using the custom AmpliSeq panel (ThermoFisher), according to manufacturer's protocols. Briefly, after PCR-based target amplification and digestion of primer sequences, Ion P1 adaptors and Ion Xpress barcodes were ligated to the amplified products. The barcoded libraries were purified using the Agencourt AMPure XP kit (Beckman Coulter Genomics) and washed with 70% ethanol before PCR-based library amplification. Libraries were quantified using Tapestation (Agilent), and subsequently pooled. Emulsion PCR was carried out using the Ion PGM Template OT2 200 Kit on OneTouch 2 System (both from ThermoFisher) according to manufacturer's protocol. Prepared templates (bead-bound DNAs) were loaded onto an Ion 316 Chip V2, and sequenced using the Ion PGM Sequencing 200 Kit v2 on an Ion PGM (all from ThermoFisher). Raw sequences (FASTQ files) were separated by bar-code and aligned to the human genome reference sequence (assembly GRCh37/hg19) by the Torrent Server (ThermoFisher). Aligned sequence (BAM) files were submitted to the Torrent Variant Caller for variant calling v5.0.3 (ThermoFisher). Called variants were subsequently annotated, filtered and visualized using Highlander. All variants were filtered against public databases (dbSNP137, 1000 Genomes and ExAC) and against our own database. We retained variants causing premature stop-codons, reading frame shifts, consensus splice site alterations or predicted damaging by at least four softwares. The mutations were subsequently confirmed and the segregation checked in each family by Sanger sequencing.

EXPRESSION OF WILD TYPE AND MUTANT EPHB4. EGFP-*EPHB4* cDNA vector (OriGene) was used to introduce 4 damaging variants (p.E664L; p.C845R; p.R838W and p.R864W) using the QuikChange Site directed Mutagenesis Kit (Agilent), according to the manufacturer's instructions. COS-7 Cells were transiently transfected with jetPEI reagent (Polyplus Transfection), according to the manufacturer's guidelines. Cells were pre-treated or not for 15h, with 50 µM of chloroquine (Sigma), an inhibitor of endosome-lysosome acidification or with 1 µM of MG132 (Sigma), a proteasome inhibitor. Cells were lysed in lysis buffer (50 mM HEPES, pH 7.4, 150 mM NaCl, 1% Triton X-100, 5 mM EGTA) buffer containing phosphatase inhibitors (1 mM sodium orthovanadate and 1 mM NaF) and a proteinase inhibitor cocktail (Roche). Cell lysates were subjected to immunoblotting to assess protein expression. Antibodies used were: monoclonal anti-β-actin (#A5441, Sigma-Aldrich) and rabbit polyclonal anti-EPHB4 (#14960, Cell Signaling Technology, Inc.).

IMMUNOFLUORESCENCE. COS-7 cells were used to express EGFP-EPHB4 wild type or each one of the 4 mutants on glass coverslips in six-well plates. After transfection, cells were washed, fixed with 4% paraformaldehyde, incubated at room temperature for 30 min and treated with buffer containing 0.1 M glycine in PBS (pH 7.4) and 0.3% Triton X-100. For fluorescence imaging, Axiovert confocal microscope (Zeiss, Oberkochen, Germany) coupled to a MRC1024 confocal scanning laser equipment (Bio-Rad, Richmond, CA), was used.

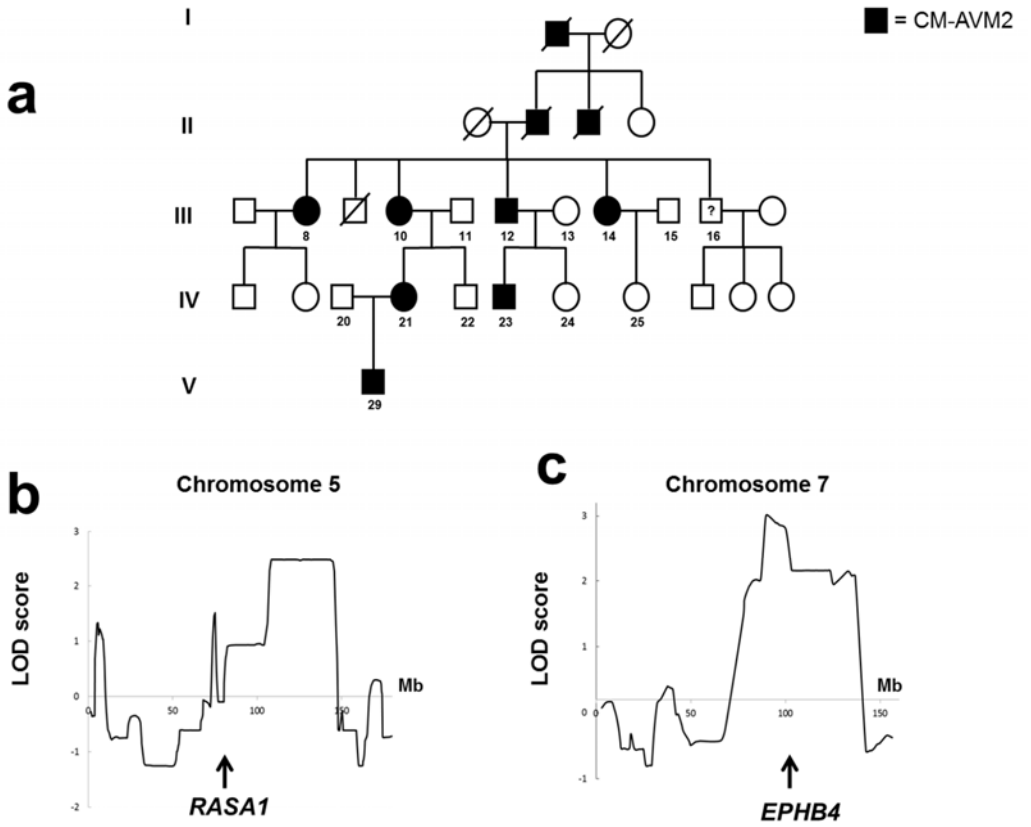

Supplementary Figure. 1: Linkage study on CM-13-HO.

Pedigree of family (CM-13-HO) used for genome-wide linkage analysis. Numbered subjects were included for genome-wide SNP-genotyping. Black symbol = affected (**a**). Result of multipoint parametric-linkage analysis results for chromosomes 5 (**b**) and 7 (**c**). X axis, chromosomal position in megabases (Mb); y axis, corresponding LOD score. Arrows, *RASA1* and *EPHB4* locations in (**b**) and (**c**), respectively.

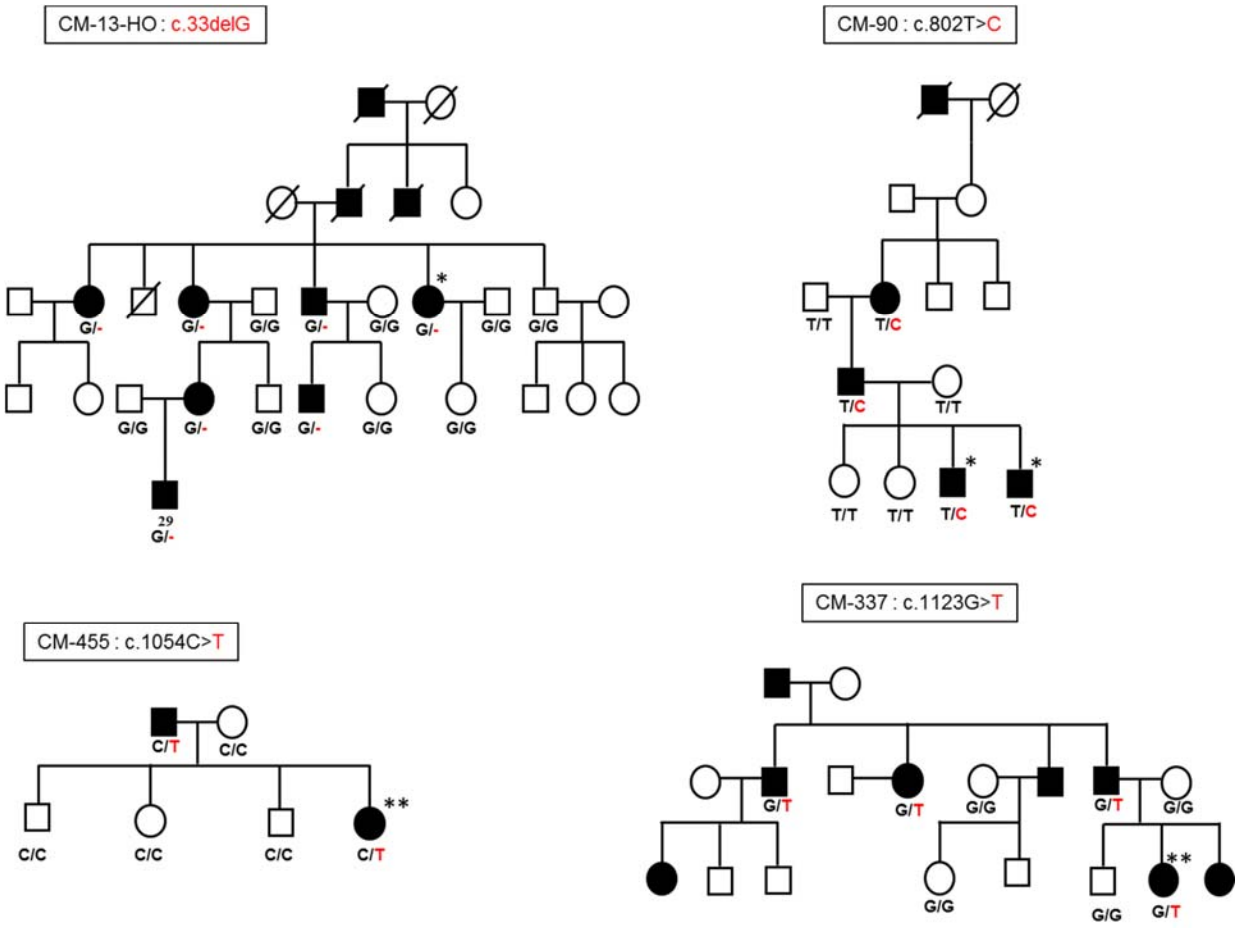

1

2 **Supplementary Figure 2. Four families showing co-**

3 **segregation of their EPHB4 mutation with CM-AVM2.**

4 * patient screened by whole exome sequencing. ** patient screened by targeted gene sequencing.

5 Segregation of the mutation checked by Sanger sequencing. Black symbol = affected. Mutant

6 allele in red.

7

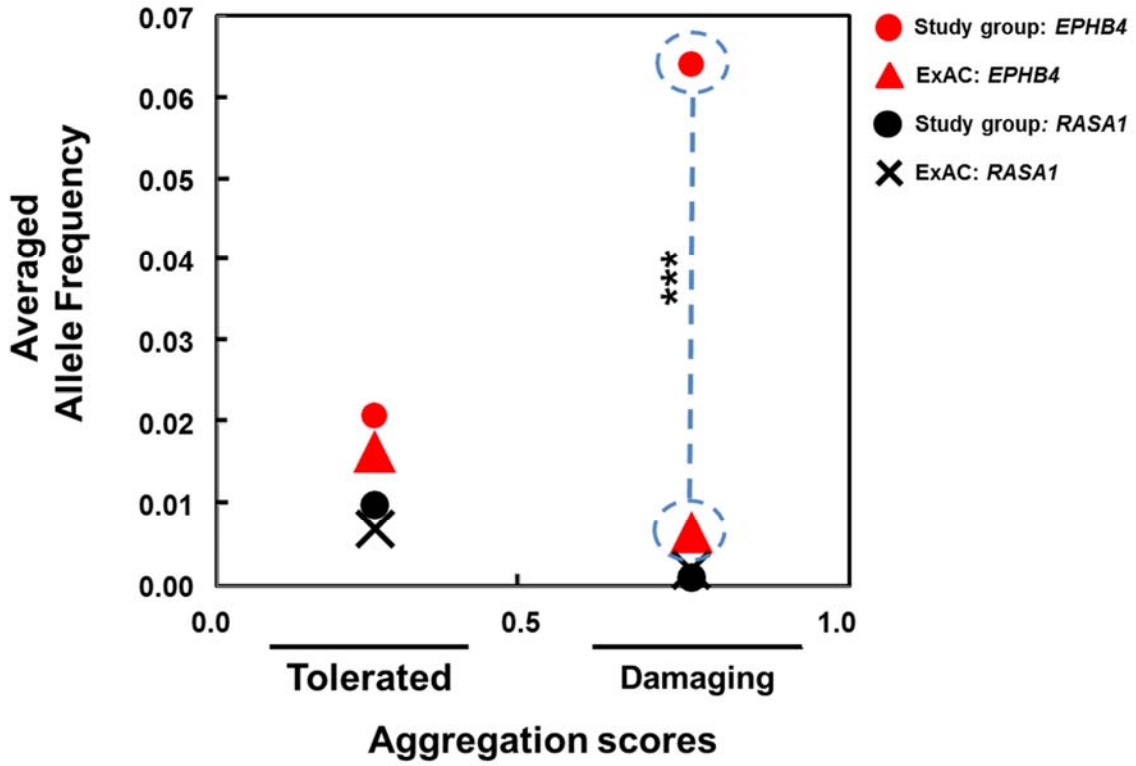

Supplementary Figure 3 : Rare damaging variants enriched in EPHB4. Averaged allele frequencies of rare non-synonymous tolerated (aggregation scores: 0 - 0.49) and damaging (aggregation scores: 0.5 – 1) variants within *EPHB4* and *RASA1* calculated for Caucasians in our study group (n=359; 79.6%) and in the ExAC database (n=33,370; 55%). To evaluate genetic burden, a "2-sample test for equality of proportions with continuity correction" was performed. Significant burden observed for *EPHB4* (****p-value* < 0.0001) and not significant for *RASA1* (*p-value* = 0.257).

Filters used	CM-13-HO-II-6A	10 affected patients
Total number of variants	57018	761385
NSV, SSV and indels	11367	132057
NOT in dbSNP and 1000G Database	382	3162
NOT in internal Database of 450 unrelated exomes	316	2124
Consensus prediction ≥ 6	41	760
Regarding the 2 linked loci:		
Variants	3	27
Shared variants in affected sibling pair CM-90	-	4
Shared variants in affected sibling pair CM-433	-	8
Genes with variants in CM-13, CM-90 and CM-433	1	1
Number of other families with a variant in gene above	-	2 (CM-291, CM-297)
Number of distinct variants in gene above	1	3
Shared gene	*EPHB4*	*EPHB4*

NSV = Non-synonymous variants; SSV = Splice-site variants; Indels = Insertions/Deletions; Consensus_prediction ≥ 6; Functional predictions retrieved from dbNSFP4.1 (damaging in SIFT, deleterious in LRT, high or medium in Mutation Assessor, damaging in Fathmm, disease-causing in Mutation Taster, and a score > 0.5 in Polyphen2).

Supplementary Table 1: Variant prioritization strategy used for whole exome sequencing data.

Prioritization strategy of variants detected by whole exome sequencing. Successive numbers correspond to variants that met each criterion. Data shown for combined analysis for one CM-13-

HO family member (II-6A) (left column) and for 8 other families, two of which had 2 patients sequenced (right column). For mutations, see Table 1.